

Optical absorption of an interacting many-polaron gas

J. Tempere and J. T. Devreese

Departement Natuurkunde, Universiteit Antwerpen (UIA), Universiteitsplein 1, B2610 Antwerpen, Belgium

(Received 26 April 2000; revised manuscript received 20 November 2000; published 6 August 2001)

The optical absorption of a many (continuum) polaron gas is derived in the framework of a variational approach at zero temperature and weak electron-phonon coupling strength. We derive a compact formula for the optical conductivity of the many-polaron system, taking into account many-body effects in the electron or hole system. Within the method presented here, these effects are contained completely in the dynamical structure factor of the electron or hole system. This allows one to build on well-established studies of the interacting electron gas. Based on this approach a feature in the absorption spectrum of the many-polaron gas, related to the emission of a plasmon together with a phonon, is identified. As an application and illustration of the technique, we compare the theoretical many-polaron optical absorption spectrum as derived in the present work with the “*d*-band” absorption feature in $\text{Nd}_2\text{CuO}_{4-\delta}$ ($\delta < 0.004$). Similarities are shown between the theoretically and the experimentally derived first frequency moment of the optical absorption of a family of differently doped $\text{Nd}_{2-x}\text{Ce}_x\text{CuO}_4$ materials.

DOI: 10.1103/PhysRevB.64.104504

PACS number(s): 74.25.Gz, 71.38.-k, 74.25.Jb

I. INTRODUCTION

As is the case for polar semiconductors and ionic crystals,¹ insight into the nature of polarons in high-temperature superconductors can be gained by studying the optical properties of these materials. The goal of the present paper is to present a theory of the optical conductivity of a system of continuum polarons at any density, including many-body effects between the constituent charge carriers, for small electron-phonon coupling constant and for zero temperature. The method we develop here is based on the variational method introduced by Lemmens, Devreese, and Brosens² (LDB) for the ground-state energy of the many-polaron gas. The advantage of this approach over other theories of many-polaron optical absorption^{3,4} is that it allows one to include many-body effects in the system of the constituent charge carriers of the polaron gas on the level of the dynamical structure factor of the underlying electron (or hole) system. Thus it is possible to select the level of approximation used in the treatment of the many-polaron gas by choosing the appropriate expression of the dynamical structure factor for the *electron* (or hole) system.

Recently the infrared spectrum of cuprates has been the subject of intensive investigations,⁵⁻¹³ especially in the case of the neodymium-cerium cuprate family $\text{Nd}_{2-x}\text{Ce}_x\text{CuO}_4$ (NCCO).^{5,8-13} Several optical absorption features in the infrared cuprate spectrum have been tentatively associated with large polarons^{7,14} or with a mixture of large and small (bi)polarons.^{15,16} These comparisons with polaron theory were derived using a single-polaron picture, so that the density (doping) dependence of the optical absorption spectra could not be studied in detail. The many-body theory of the *N*-polaron spectrum, presented here, allows one to study the density (doping) dependence of optical absorption spectra. As a first application of the many-polaron optical absorption theory introduced here, a preliminary comparison is presented between the theoretical many-polaron optical absorption derived in the current work and the midinfrared spec-

trum of the neodymium-cerium cuprates recently determined experimentally by Lupi *et al.*⁵

II. OPTICAL ABSORPTION IN THE MANY-POLARON SYSTEM

A. LDB variational wave function for a many-polaron system

The Hamiltonian of a system of *N* interacting continuum polarons is given by

$$H_0 = \sum_{j=1}^N \frac{p_j^2}{2m_b} + \sum_{\mathbf{k}} \hbar \omega_{\text{LO}} a_{\mathbf{k}}^\dagger a_{\mathbf{k}} + \sum_{\mathbf{k}} \sum_{j=1}^N [e^{i\mathbf{k}\cdot\mathbf{r}_j} a_{\mathbf{k}} V_{\mathbf{k}} + e^{-i\mathbf{k}\cdot\mathbf{r}_j} a_{\mathbf{k}}^\dagger V_{\mathbf{k}}^*] + \frac{e^2}{2\epsilon_\infty} \sum_{j=1}^N \sum_{l(\neq j)=1}^N \frac{1}{|\mathbf{r}_l - \mathbf{r}_j|}, \quad (1)$$

where \mathbf{r}_j and \mathbf{p}_j represent the position and momentum of the *N* constituent electrons (or holes) with band mass m_b , $a_{\mathbf{k}}^\dagger$, and $a_{\mathbf{k}}$ denote the creation and annihilation operators for longitudinal optical (LO) phonons with wave vector \mathbf{k} and frequency ω_{LO} , $V_{\mathbf{k}}$ describes the amplitude of the interaction between the electrons and the phonons; and e is the elementary electron charge. The ground-state energy of this many-polaron Hamiltonian has been studied before by LDB,² for small electron-phonon coupling, by introducing a variational wave function

$$|\psi_{\text{LDB}}\rangle = U|\phi\rangle|\varphi_{\text{el}}\rangle, \quad (2)$$

where $|\varphi_{\text{el}}\rangle$ represents the ground-state many-body wave function for the electron (or hole) system and $|\phi\rangle$ is the phonon vacuum, and U is a many-body unitary operator which determines a canonical transformation for a fermion gas interacting with a boson field:

$$U = \exp \left\{ \sum_{j=1}^N \sum_{\mathbf{k}} (f_{\mathbf{k}} a_{\mathbf{k}} e^{i\mathbf{k}\cdot\mathbf{r}_j} - f_{\mathbf{k}}^* a_{\mathbf{k}}^\dagger e^{-i\mathbf{k}\cdot\mathbf{r}_j}) \right\}. \quad (3)$$

In the limit of one fermion, U reduces to a canonical transformation inspired by Tomonaga¹⁷ and applied later by several workers, after Lee, Low, and Pines,¹⁸ but always for one-particle theories. In LDB,² this canonical transformation was extended and used to establish a many-fermion theory. The $f_{\mathbf{k}}$ were determined variationally,² resulting in

$$f_{\mathbf{k}} = \frac{V_{\mathbf{k}}}{\hbar \omega_{LO} + \frac{\hbar^2 k^2}{2m_b S(\mathbf{k})}}, \quad (4)$$

for a system with total momentum $\mathbf{P} = \sum_j \mathbf{p}_j = 0$. In this expression, $S(\mathbf{k})$ represents the static structure factor of the constituent interacting many electron or hole system:

$$NS(\mathbf{k}) = \left\langle \sum_{j=1}^N \sum_{j'=1}^N e^{i\mathbf{k} \cdot (\mathbf{r}_j - \mathbf{r}_{j'})} \right\rangle. \quad (5)$$

The angular brackets $\langle \dots \rangle$ represent the expectation value with respect to the ground state. It may be emphasized that Eq. (3), although it appears like a straightforward generalization of the one-particle transformation in Ref. 17, represents—especially in its implementation—a nontrivial extension of a one-particle approximation to a many-body system. As noted in the Introduction, the main advantage of the LDB many-polaron variational approach lies in the fact that the many-body effects in the system of charge carriers (electrons or holes) are completely contained in the structure factor of the electron (or hole) gas. This advantage will be carried through into the calculation of the optical properties of the interacting gas of continuum polarons which is the subject of the current paper.

B. Kubo formula for the optical conductivity of the many-polaron gas

The many-polaron optical conductivity is the response of the current density, in the system described by the Hamiltonian (1), to an applied electric field (along the x axis) with frequency ω . This applied electric field introduces a perturbation term in the Hamiltonian (1), which couples the vector potential of the incident electromagnetic field to the current density. As is well known, within linear response theory, the optical conductivity can be expressed through the Kubo formula as a current-current correlation function:¹⁹

$$\text{Re}[\sigma(\omega)] = \frac{1}{V\hbar\omega^3} \frac{e^2}{m_b^2} \text{Re} \left\{ \sum_{\mathbf{k}, \mathbf{k}'} k_x \cdot k'_x \int_0^\infty e^{i\omega t} \left\langle \left[\begin{array}{l} e^{iH_0 t/\hbar} (\rho_{\mathbf{k}} a_{\mathbf{k}} V_{\mathbf{k}} + \rho_{-\mathbf{k}} a_{\mathbf{k}}^+ V_{\mathbf{k}}^*) e^{-iH_0 t/\hbar}, \\ (\rho_{\mathbf{k}'} a_{\mathbf{k}'} V_{\mathbf{k}'} + \rho_{-\mathbf{k}'} a_{\mathbf{k}'}^+ V_{\mathbf{k}'}^*) \end{array} \right] \right\rangle dt \right\}. \quad (11)$$

Up to this point, no approximations other than *linear response theory* have been made.

C. LDB canonical transformation for the optical conductivity

The expectation value appearing on the right-hand side of expression (11) for the real part of the optical conductivity is calculated now with respect to the LDB many-polaron wave function $|\psi_{\text{LDB}}\rangle$ (2):

$$\mathcal{J}(\mathbf{k}, \mathbf{k}') = \langle \psi_{\text{LDB}} | [e^{iH_0 t/\hbar} (\rho_{\mathbf{k}} a_{\mathbf{k}} V_{\mathbf{k}} + \rho_{-\mathbf{k}} a_{\mathbf{k}}^+ V_{\mathbf{k}}^*) e^{-iH_0 t/\hbar}, (\rho_{\mathbf{k}'} a_{\mathbf{k}'} V_{\mathbf{k}'} + \rho_{-\mathbf{k}'} a_{\mathbf{k}'}^+ V_{\mathbf{k}'}^*)] | \psi_{\text{LDB}} \rangle \quad (12)$$

$$\sigma(\omega) = i \frac{Ne^2}{Vm_b\omega} + \frac{1}{V\hbar\omega} \int_0^\infty e^{i\omega t} \langle [J_x(t), J_x(0)] \rangle dt. \quad (6)$$

In this expression, V is the volume of the system, and J_x is the x component of the current operator \mathbf{J} , which is related to the momentum operators of the charge carriers:

$$\mathbf{J} = \frac{q}{m_b} \sum_{j=1}^N \mathbf{p}_j = \frac{q}{m_b} \mathbf{P}, \quad (7)$$

with q the charge of the charge carriers ($+e$ for holes, $-e$ for electrons) and \mathbf{P} the total momentum operator of the charge carriers. The real part of the optical conductivity at temperature zero, which is proportional to the optical absorption coefficient, can be written as a function of the total momentum operator of the charge carriers as follows:

$$\text{Re}[\sigma(\omega)] = \frac{1}{V\hbar\omega} \frac{e^2}{m_b^2} \text{Re} \left\{ \int_0^\infty e^{i\omega t} \langle [P_x(t), P_x(0)] \rangle dt \right\}. \quad (8)$$

Integrating by parts twice, the real part of the optical conductivity of the many-polaron system can be written with a force-force correlation function:

$$\text{Re}[\sigma(\omega)] = \frac{1}{V\hbar\omega^3} \frac{e^2}{m_b^2} \text{Re} \left\{ \int_0^\infty e^{i\omega t} \langle [F_x(t), F_x(0)] \rangle dt \right\}, \quad (9)$$

with $\mathbf{F} = (i/\hbar)[H_0, \mathbf{P}]$. The commutator of the Hamiltonian (1) with the total momentum operator of the charge carriers simplifies to

$$\mathbf{F} = -i \sum_{\mathbf{k}} \sum_{j=1}^N \mathbf{k} (e^{i\mathbf{k} \cdot \mathbf{r}_j} a_{\mathbf{k}} V_{\mathbf{k}} + e^{-i\mathbf{k} \cdot \mathbf{r}_j} a_{\mathbf{k}}^+ V_{\mathbf{k}}^*). \quad (10)$$

This result for the force operator clarifies the significance of using the force-force correlation function rather than the momentum-momentum correlation function. The operator product $F_x(t)F_x(0)$ is proportional to $|V_{\mathbf{k}}|^2$, the charge-carrier—phonon interaction strength. This will be a distinct advantage for any expansion of the final result in the charge-carrier—phonon interaction strength, since one power of $|V_{\mathbf{k}}|^2$ is factored out beforehand. Denoting $\rho_{\mathbf{k}} = \sum_{j=1}^N e^{i\mathbf{k} \cdot \mathbf{r}_j}$, the real part of the optical conductivity takes the form

$$= \left\langle \varphi_{\text{el}} \left| \left\langle \phi \left| \left[\begin{array}{c} e^{iH't/\hbar} U^{-1} (\rho_{\mathbf{k}} a_{\mathbf{k}} V_{\mathbf{k}} + \rho_{-\mathbf{k}} a_{\mathbf{k}}^+ V_{\mathbf{k}}^*) U e^{-iH't/\hbar}, \\ U^{-1} (\rho_{\mathbf{k}'} a_{\mathbf{k}'} V_{\mathbf{k}'} + \rho_{-\mathbf{k}'} a_{\mathbf{k}'}^+ V_{\mathbf{k}'}^*) U \end{array} \right] \right| \phi \right\rangle \right| \varphi_{\text{el}} \right\rangle, \quad (13)$$

where U is the many-polaron canonical transformation defined in Eq. (3) and $H' = U^{-1} H_0 U$ is the transformed Hamiltonian obtained in Ref. 2. The canonical transformation of the force term is

$$U^{-1} (\rho_{\mathbf{k}} a_{\mathbf{k}} V_{\mathbf{k}} + \rho_{-\mathbf{k}} a_{\mathbf{k}}^+ V_{\mathbf{k}}^*) U = \rho_{\mathbf{k}} (a_{\mathbf{k}} - f_{\mathbf{k}}^* \rho_{-\mathbf{k}}) V_{\mathbf{k}} + \rho_{-\mathbf{k}} (a_{\mathbf{k}}^+ - f_{\mathbf{k}} \rho_{\mathbf{k}}) V_{\mathbf{k}}^*. \quad (14)$$

The terms of lowest order in the electron-phonon interaction amplitude $|V_{\mathbf{k}}|^2$ are given by

$$\mathcal{J}(\mathbf{k}, \mathbf{k}') = |V_{\mathbf{k}}|^2 \delta_{\mathbf{k}\mathbf{k}'} \langle \varphi_{\text{el}} | \langle \phi | e^{iH't/\hbar} \rho_{\mathbf{k}} a_{\mathbf{k}} e^{-iH't/\hbar} \rho_{-\mathbf{k}} a_{\mathbf{k}}^+ - \rho_{\mathbf{k}} a_{\mathbf{k}} e^{iH't/\hbar} \rho_{-\mathbf{k}} a_{\mathbf{k}}^+ e^{-iH't/\hbar} | \phi \rangle | \varphi_{\text{el}} \rangle \quad (15)$$

$$= 2i |V_{\mathbf{k}}|^2 \delta_{\mathbf{k}\mathbf{k}'} \text{Im} [\langle \varphi_{\text{el}} | \langle \phi | e^{iH't/\hbar} \rho_{\mathbf{k}} a_{\mathbf{k}} e^{-iH't/\hbar} \times \rho_{-\mathbf{k}} a_{\mathbf{k}}^+ | \phi \rangle | \varphi_{\text{el}} \rangle]. \quad (16)$$

Taking the expectation value with respect to the phonon vacuum, we find

$$\mathcal{J}(\mathbf{k}, \mathbf{k}') = 2i |V_{\mathbf{k}}|^2 \delta_{\mathbf{k}\mathbf{k}'} \times \text{Im} \{ e^{-i\omega_{\text{LO}} t} \langle \varphi_{\text{el}} | e^{iH't/\hbar} \rho_{\mathbf{k}} e^{-iH't/\hbar} \rho_{-\mathbf{k}} | \varphi_{\text{el}} \rangle \}. \quad (17)$$

This can be substituted in the expression (11) for the real part of the optical conductivity, which becomes

$$\text{Re}[\sigma(\omega)] = -2 \frac{1}{\sqrt{\hbar} \omega^3} \frac{e^2}{m_b^2} \text{Im} \left\{ \sum_{\mathbf{k}} k_x^2 |V_{\mathbf{k}}|^2 \int_0^\infty e^{i\omega t} \text{Im} \times [e^{-i\omega_{\text{LO}} t} \langle \varphi_{\text{el}} | e^{iH't/\hbar} \rho_{\mathbf{k}} e^{-iH't/\hbar} \rho_{-\mathbf{k}} | \varphi_{\text{el}} \rangle] dt \right\}. \quad (18)$$

The right-hand side of Eq. (18) can be written in a more compact form by introducing the dynamical structure factor of the electron (or hole) system.

D. General expression

To find the formula for the real part of the optical conductivity in its final form, we introduce the standard expression for the dynamical structure factor of the system of charge carriers interacting through a Coulomb potential,

$$S(\mathbf{q}, \omega) = \int_{-\infty}^{+\infty} \left\langle \varphi_{\text{el}} \left| \frac{1}{2} \sum_{j,j'} e^{i\mathbf{q} \cdot [\mathbf{r}_j(t) - \mathbf{r}_{j'}(0)]} \right| \varphi_{\text{el}} \right\rangle e^{i\omega t} dt. \quad (19)$$

Rewriting expression (18) with the dynamical structure factor of the electron (or hole) gas results in

$$\text{Re}[\sigma(\omega)] = \frac{n}{\hbar \omega^3} \frac{e^2}{m_b^2} \sum_{\mathbf{k}} k_x^2 |V_{\mathbf{k}}|^2 S(\mathbf{k}, \omega - \omega_{\text{LO}}), \quad (20)$$

where $n = N/V$ is the density of charge carriers. As noted before, $V_{\mathbf{k}}$ is the electron-phonon interaction amplitude and k_x is the x component of the wave vector. Formula (20) for the optical absorption of the many-polaron system has an intuitively appealing form.

In the theory of one-polaron optical absorption for weak coupling constants α , the optical absorption coefficient as obtained from Fermi's golden rule is²⁰

$$\begin{aligned} \text{1 polaron: } \text{Re}[\sigma(\omega)] &\propto \omega^{-3} \sum_{\mathbf{k}} k_x^2 |V_{\mathbf{k}}|^2 \\ &\times \delta[\hbar k^2 / (2m_b) - (\omega - \omega_{\text{LO}})]. \end{aligned} \quad (21)$$

At low densities, the dynamical structure factor $S(q, \nu)$ is strongly peaked around $q^2/2 = \nu$ and is close to zero everywhere else.²¹ Substituting a δ function $\delta(q^2/2 - \nu)$ for the dynamical structure factor in formula (20) it is easily seen that the one-polaron limit (21) (Ref. 20) is retrieved. The one-polaron result (21) is derived²⁰ by considering a process in which the initial state consists of a photon of energy $\hbar \omega$ and a polaron in its ground state, and the final state consists of an emitted LO phonon with energy $\hbar \omega_{\text{LO}}$ and the polaron, scattered into a state with momentum \mathbf{k} and kinetic energy $(\hbar k)^2 / (2m_b) = \hbar(\omega - \omega_{\text{LO}})$. The many-polaron result, formula (20), is a generalization of this one-polaron picture. The contribution which corresponds to the scattering of a polaron into the momentum state \mathbf{k} and energy $\hbar(\omega - \omega_{\text{LO}})$ is now weighed by the dynamical structure factor $S(k, \omega - \omega_{\text{LO}})$ of the electron (or hole) gas.

Formula (20) is reminiscent of the Hopfield formula²² describing the effect of impurities on the optical absorption of metals, which in turn is related to the expression obtained by Ron and Tzoar²³ for the optical absorption in a quantum plasma. Formula (20) also represents a generalization of the results obtained by Gurevich, Lang, and Firsov.²⁴ These authors focused their attention on the many-body effects related to the Fermi exclusion statistics, whereas the present analysis will extend the results of Ref. 24 to study the influence of plasmons and further many-body effects in the system of the constituent electrons or holes, as discussed in the next section.

The advantage of the LDB canonical transformation method² for the evaluation of the *ground-state energy* of a polaron gas is that the many-body effects are contained in the *static* structure factor of the electron (or hole) system, ap-

TABLE I. Material parameters used in the various figures. The physical parameters for GaAs correspond to those of the GaAs-AlGaAs heterostructure (Ref. 28), the material parameters for ZnO are taken from Ref. 29. The physical parameters for the neodymium-cerium cuprate are taken from Refs. 8 and 30. “n.a.” (“not applicable”) means that not enough data are available to estimate this material parameter.

Material parameters		GaAs	ZnO	Nd _{1.85} Ce _{0.15} CuO ₄
Phonon frequency	$\hbar\omega_{\text{LO}}=$	36.77 meV	73.27 meV	74 meV
Dielectric constants	$\epsilon_0=$	12.83	8.15	n.a.
	$\epsilon_\infty=$	10.9	4.00	ca. 3.
Band mass	$m_b=$	0.0657 m_e	0.24 m_e	n.a.
Coupling constant	$\alpha=$	0.068	0.849	n.a.
Polaron length unit	$a_{\text{HO}}=$	5.616 nm	2.082 nm	n.a.
Bohr radius	$a_B=$	8.7797 nm	0.882 nm	n.a.

appearing in the analytical expression for the energy. The corresponding advantage of the canonical transformation in the present case, for the optical conductivity, is that many-body effects are again incorporated through a structure factor, now the dynamical structure factor of the electron (or hole) system. The level of approximation made in treating the many-body nature of the polaron system is determined by the choice of the dynamical structure factor of the electron or hole system.

In the present treatment of the electron-phonon interactions, the terms to leading order in $|V_{\mathbf{k}}|^2$ are automatically taken into account through the variational formulation based on LDB.² As noted before, the use of the force-force correlation function allows one to express the real part of the optical conductivity as $\text{Re}[\sigma(\omega)] = \alpha \mathcal{F}(\omega, \alpha)$, so that to lowest order in α , $\text{Re}[\sigma(\omega)] = \alpha \mathcal{F}(\omega, \alpha=0)$ where the electron-phonon interaction is no longer present in the factor \mathcal{F} which includes the many-body effects of the electron (or hole) system. A possible way to take into account higher-order terms in the electron-phonon interactions would be to include electron-phonon coupling effects at the level of the dynamical structure factor appearing in \mathcal{F} , in a manner similar to Mahan’s treatment of the polaron spectral function,²⁵ or to include multiple-phonon final states in the calculation.²⁶

E. Scaling relation for the optical absorption in two and three dimensions

The modulus squared of the Fröhlich electron-phonon interaction amplitude is given by

$$|V_{\mathbf{k}}|^2 = \begin{cases} \frac{(\hbar\omega_{\text{LO}})^2}{k^2} \frac{4\pi\alpha}{V} \sqrt{\frac{\hbar}{2m_b\omega_{\text{LO}}}} & \text{in 3D,} \\ \frac{(\hbar\omega_{\text{LO}})^2}{k} \frac{2\pi\alpha}{A} \sqrt{\frac{\hbar}{2m_b\omega_{\text{LO}}}} & \text{in 2D,} \end{cases} \quad (22)$$

where α is the (dimensionless) Fröhlich coupling constant determining the coupling strength between the charge carriers and the longitudinal optical phonons, and A is the surface of the 2D system.²⁷ In what follows, we will use polaron units ($\hbar = m_b = \omega_{\text{LO}} = 1$). The sum over wave vectors in Eq. (20) can be written as an integral, so that for the three dimensional case (with dynamical structure factor S_{3D}) we find

$$\text{Re}[\sigma_{3D}(\omega)] = ne^2 \frac{2}{3} \alpha \frac{1}{2\pi\omega^3} \int_0^\infty dq q^2 S_{3D}(q, \omega - \omega_{\text{LO}}), \quad (23)$$

and for the two-dimensional case

$$\text{Re}[\sigma_{2D}(\omega)] = ne^2 \frac{\pi}{2} \alpha \frac{1}{2\pi\omega^3} \int_0^\infty dq q^2 S_{2D}(q, \omega - \omega_{\text{LO}}). \quad (24)$$

From these expressions, it is clear that the scaling relation

$$\text{Re}[\sigma_{2D}(\omega, \alpha)] = \text{Re}[\sigma_{3D}(\omega, 3\pi\alpha/4)], \quad (25)$$

which holds for the one-polaron case introduced in Ref. 27, is also valid for the many-polaron case if the corresponding 2D or 3D dynamical structure factor is used.

III. RESULTS AND DISCUSSION

A. General results

The expressions (23) and (24) allow us to derive results both for a three-dimensional and for a two-dimensional polaron gas at $T=0$. The choice of a dynamical structure factor for the electron (or hole) system allows one furthermore to study the different levels of approximation [Hartree-Fock, random phase approximation (RPA), etc.] in the treatment of the many-electron or many-hole system. The results presented in this section were obtained using the material parameters of GaAs [for the two-dimensional (3D) case] and ZnO (for the three-dimensional case). These material parameters^{8,28–30} are summarized in Table I.

Figure 1 shows the Hartree-Fock and the RPA result for the 2D many-polaron optical absorption spectrum (for GaAs, at a density $n = 10^{12} \text{ cm}^{-2}$). For reference, the dashed curve represents the familiar one-polaron result. In a first step, we discuss the result obtained by using the Hartree-Fock expression for the dynamical structure factor of the electron (or hole) system in the expressions (23) and (24).

The Fermi statistics causes the polarons to fill up a Fermi sphere up to $k_F = [n/(2\pi)]^{1/2}$. The optical absorption of the polaron gas resulting from this system is represented by the solid curve labeled “Hartree-Fock” in Fig. 1. The spectral weight at frequencies between ω_{LO} and $1.4\omega_{\text{LO}}$ in Fig. 1 is

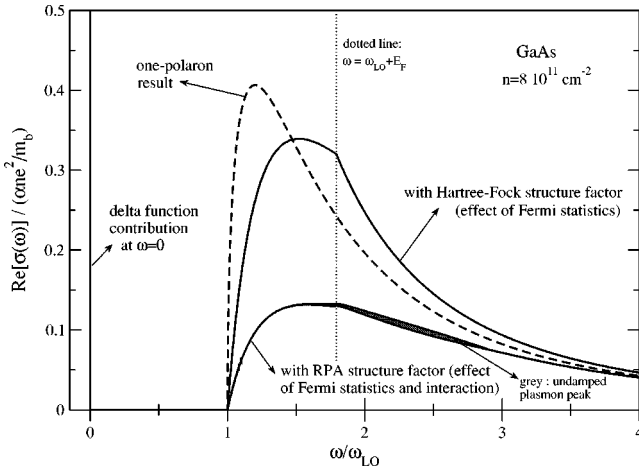


FIG. 1. The real part of the optical conductivity (proportional to the optical absorption coefficient) of an interacting large-polaron gas is shown as a function of frequency, for a two-dimensional gas (GaAs) from Eq. (24). The material parameters are given in Table I. The dashed curve represents the one-polaron result, the solid curve labeled “Hartree-Fock structure factor” shows the result using the Hartree-Fock approximation to the dynamical structure factor of the electron (hole) system, and the solid curve labeled “RPA structure factor” is the result in the random phase approximation. The dotted vertical line indicates the threshold frequency above which all polarons can be scattered into unoccupied final states and participate in the absorption process. The broad gray peak in the RPA curve is the plasmon-phonon contribution (see also Fig. 2).

reduced as compared to the single-polaron case, whereas at higher frequencies it is enhanced. A kink appears in the spectrum at $\omega = \omega_{LO} + E_F/\hbar$, as indicated by the dotted vertical line in Fig. 1.

This can be understood as follows. The absorption process is characterized by an *initial* state consisting of a polaron gas filling up the Fermi sphere (up to energy E_F , at $T=0$) and a photon with given energy $\hbar\omega$, and by a *final* state made up of an emitted LO phonon with energy $\hbar\omega_{LO}$ and a polaron gas such that the one-polaron state inside the Fermi sphere is not occupied and the one-polaron state with energy $E > E_F$ is occupied. The incident photon can only excite polarons out of the Fermi sea for which $\hbar\omega > \hbar\omega_{LO} + E_F$. A straightforward calculation in 2D shows that the fraction of polaron states in the Fermi sphere which can interact with a photon of energy $\hbar\omega$ is given by

$$\begin{cases} 0 & \text{for } \omega < \omega_{LO}, \\ \frac{\hbar(\omega - \omega_{LO})}{E_F} & \text{for } \omega_{LO} < \omega < E_F/\hbar + \omega_{LO}, \\ 1 & \text{for } \omega > E_F/\hbar + \omega_{LO}. \end{cases} \quad (26)$$

For photon frequencies between ω_{LO} and $\omega_{LO} + E_F/\hbar$, the number of polarons which cannot participate in the optical absorption process due to the Pauli exclusion principle decreases linearly. At $\omega = \omega_{LO} + E_F/\hbar$, all polarons can participate. This leads to a kink in the function (26) describing the number of polarons which can interact with the photon of given energy $\hbar\omega$, as a function of ω . This is also the origin

of the kink in the optical absorption. This kink in the 2D many-polaron optical absorption spectrum at $\hbar\omega = \hbar\omega_{LO} + E_F$ was already noted in Ref. 28.

The solid curve labeled “RPA” in Fig. 1 is obtained by using the RPA for the dynamical structure factor of the electron (or hole) system. It illustrates the combined effects of the Fermi statistics, discussed in the previous paragraph, and screening in the electron (or hole) system. In comparison to the Hartree-Fock curve, the main effect is an overall reduction of the spectral weight at frequencies $\omega > \omega_{LO}$. There is, however, a second effect, which is the appearance of a contribution related to plasmons—this is the subject of the next subsection.

B. Plasmon-phonon contribution

The RPA dynamical structure factor for the electron (or hole) system can be separated in two parts, one related to continuum excitations of the electrons (or holes) S_{cont} and one related to the undamped plasmon branch:³¹

$$S_{RPA}(q, \omega) = A_{pl}(q) \delta[\omega - \omega_{pl}(q)] + S_{cont}(q, \omega),$$

where $\omega_{pl}(q)$ is the wave-number-dependent plasmon frequency and A_{pl} is the strength of the undamped plasmon branch.³¹ The insets of Fig. 2 depict the regions in the q - v plane [$q = k/k_F, v = m_b\omega/(\hbar k_F^2)$] where the RPA dynamical structure factor is different from zero. The contribution [after substitution of S_{RPA} in Eqs. (23) and (24) in the many-polaron optical absorption] deriving from the undamped plasmon branch $A_{pl}(q) \delta[\omega - \omega_{pl}(q)]$ will be denoted the “*plasmon-phonon*” contribution. The physical process related to this contribution is the emission of both a phonon and a plasmon in the scattering process.

Figure 2 shows the result for the optical absorption of the many-polaron gas for the 2D case (GaAs, left panel) and the 3D case (ZnO, right panel). For reference, the dashed curves show the one-polaron result. The solid curves show the many-polaron results in the random phase approximation. The shaded gray areas indicate the plasmon-phonon contribution.

Now examine the 3D case (the right panel of Fig. 2). The frequency of the undamped plasmon mode lies between ω_1 and ω_2 where $\omega_1 = \omega_{pl} = \sqrt{4\pi n e^2/m_b}$ is the frequency of the plasmon branch at $q=0$, and ω_2 is the frequency at which the branch of the undamped plasmons enters the Landau damping region [whose edge is given by $\omega = \hbar q^2/(2m_b) + \hbar k_F q/(2m_b)$]. The corresponding plasmon-phonon contribution to the optical absorption “starts” at $\omega_{LO} + \omega_1$ and “ends” at $\omega_{LO} + \omega_2$. These frequencies are indicated by vertical dotted lines in the right panel of Fig. 2.

In the 2D case, the undamped plasmon branch is acoustic like; for $q \rightarrow 0$, $\omega_{pl} \rightarrow 0$. Consequently, the phonon-plasmon peak in this case extends from ω_{LO} up to $\omega_{LO} + \omega_2$ where ω_2 is the frequency at which the undamped plasmon branch enters the region of the continuum excitations of the 2D (RPA) electron gas.

In Fig. 3, the evolution of the many-polaron optical absorption spectrum is shown as the density of electrons (or holes) is increased. Two effects can be observed for increas-

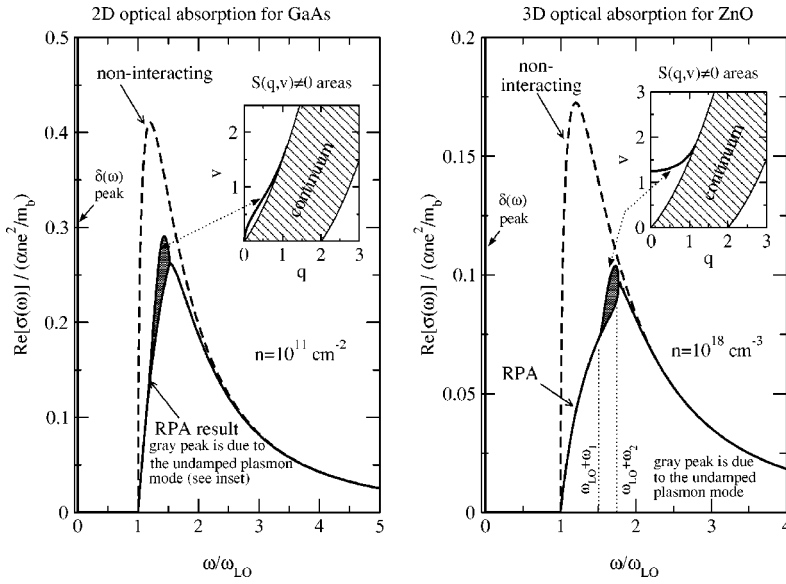


FIG. 2. The real part of the optical conductivity is shown as a function of frequency for an interacting large-polaron gas in the 2D case (left panel) and the 3D case (right panel). The material parameters used here are given in Table I. The dashed curves represent the single polaron spectra. The solid curve represents the many-polaron spectrum. In this figure, the plasmon-phonon contribution to the optical many-polaron spectrum is shown as a shaded area. This contribution arises from a process where a polaron, with the absorption of a photon, emits a phonon and a plasmon. The inset shows the regions in the $q-v$ plane where the dynamical structure factor $S(q,v)$ of the electron (or hole) system used in the optical absorption formulas (23) and (24) differs from zero; the Landau damping region and the undamped plasmon branch can be distinguished.

ing density: the reduction of the optical absorption above $\omega > \omega_{LO}$ and the shift towards higher frequencies of the plasmon-phonon contribution, both in 2D (left panel) and in 3D (right panel). The f sum rule is nevertheless satisfied due to the presence of a central $\delta(\omega)$ peak³² in the optical absorption of the polaron gas at $T=0$.

C. Comparison with other theories

In earlier work, Wu, Peeters, and Devreese²⁸ studied the influence of screening on the electron-phonon interaction in a two-dimensional electron gas based on a memory function approach using a perturbation expansion in the electron-LO-phonon coupling constant. The results of this perturbative approach of Ref. 28 for the optical conductivity in 2D, also in the RPA framework, are consistent with the results derived from the present method based on the *variational* LDB unitary transformation. These authors found an enhancement of the optical absorption at the frequency where the undamped plasmon branch reaches the region of continuum excitations

of the electron gas. The present, variational, method extends these results by taking into account the entire undamped plasmon branch.

Recently, Cataudella, De Filippis, and Iadonisi³ investigated the optical properties of the many-polaron gas by calculating the correction due to electron-phonon interactions to the RPA dielectric function of the electron gas, starting from the Feynman polaron model and Ref. 1. An aspect of the present method is that it is not restricted to the random phase approximation for the treatment of the many-body effects between the charge carriers. Cataudella *et al.*³ also find a suppression of the optical absorption with increasing density. To our knowledge, the plasmon-phonon contribution was not revealed by the work of Cataudella *et al.*³

For small (Holstein) polarons, a theory of the interacting many-polaron gas and the polaronic Wigner crystal has been developed by Fratini and Quemerais.³³ The optical absorption of the interacting system of Holstein polarons was derived,³⁴ and compared to the infrared-active modes ob-

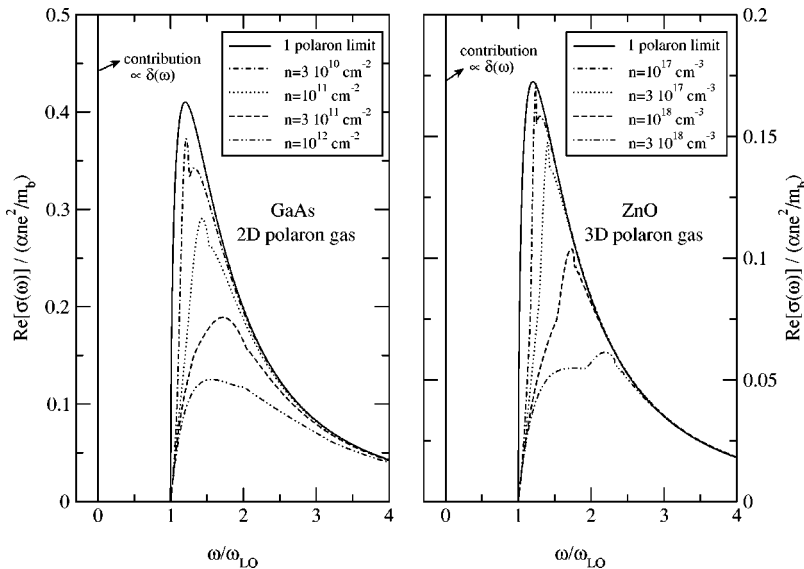


FIG. 3. The real part of the optical conductivity is shown as a function of frequency for different densities of an interacting large-polaron gas, in the 2D case (left panel) and the 3D case (right panel). The material parameters used for this figure are given in Table I. For increasing density, the optical conductivity is reduced. Another effect in the RPA approximation is the presence of a peak related to the undamped plasmon branch (see Fig. 2) which shifts according to the plasma frequency.

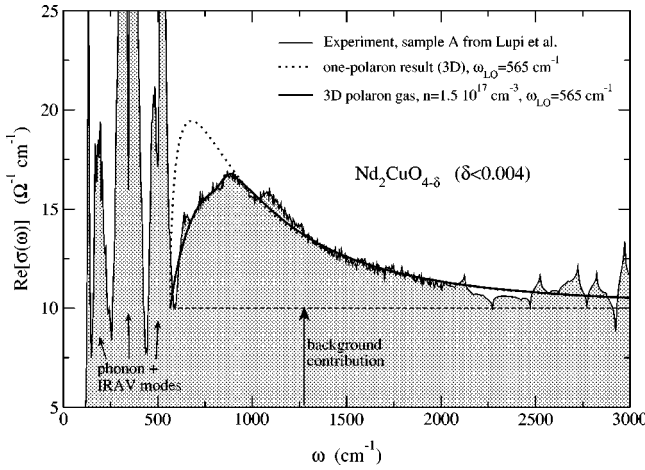


FIG. 4. The infrared absorption of $\text{Nd}_2\text{CuO}_{4-\delta}$ ($\delta < 0.004$) is shown as a function of frequency, up to 3000 cm^{-1} . The experimental results of Calvani and co-workers⁵ is represented by the thin black curve and by the shaded area. The so-called “d-band” rises in intensity around 600 cm^{-1} and increases in intensity up to a maximum around 1000 cm^{-1} . The dotted curve shows the single polaron result. The full black curve represents the theoretical results obtained in the present work for the interacting many-polaron gas with $n = 1.5 \times 10^{17} \text{ cm}^{-3}$, $\alpha = 2.1$ and $m_b = 0.5 m_e$.

served in the far-infrared spectrum of cuprate materials. The present formalism describes an interacting gas of large (Fröhlich) polarons; moreover, the structure factors (RPA and Hartree-Fock) used here to describe the electron gas or the hole gas underlying the polaron gas do not describe Wigner crystallization. Although the present formalism and the theory for the Holstein polarons describe different regimes, Eagles *et al.*¹⁶ have suggested that in cuprate materials a mixture of small and large polarons could coexist.

D. Comparison to the infrared spectrum of $\text{Nd}_{2-x}\text{Ce}_x\text{CuO}_4$

Calvani and collaborators have performed doping-dependent measurements of the infrared absorption spectra of the high- T_c material $\text{Nd}_{2-x}\text{Ce}_x\text{CuO}_4$ (NCCO). The region of the spectrum examined by these authors ($50\text{--}10\,000 \text{ cm}^{-1}$) is very rich in absorption features: they observe a “Drude-like” component at the lowest frequencies and a set of sharp absorption peaks related to phonons and infrared-active modes (IRAV, up to about 1000 cm^{-1}) possibly associated to small (Holstein) polarons.³⁴ Three distinct absorption bands can be distinguished: the “d band” (around 1000 cm^{-1}), the midinfrared band (MIR, around 5000 cm^{-1}), and the charge-transfer band (CT, around 10^4 cm^{-1}).⁸ Of all these features, the d band and, at a higher temperatures, the Drude-like component have (hypothetically) been associated with large polaron optical absorption.^{5,7,14}

For the lowest levels of Ce doping, the d band can be most clearly distinguished from the other features. The experimental optical absorption spectrum (up to 3000 cm^{-1}) of $\text{Nd}_2\text{CuO}_{4-\delta}$ ($\delta < 0.004$), obtained by Lupi *et al.*,⁵ is shown in Fig. 4 (shaded area) together with the theoretical curve obtained by the present method (solid, bold curve) and,

for reference, the one-polaron optical absorption result (dotted curve). At lower frequencies ($600\text{--}1000 \text{ cm}^{-1}$) a marked difference between the single polaron optical absorption and the many-polaron result is manifest. The experimental d band can be clearly identified, rising in intensity at about 600 cm^{-1} , peaking around 1000 cm^{-1} , and then decreasing in intensity above that frequency. At a density of $n = 1.5 \cdot 10^{17} \text{ cm}^{-3}$, we found a remarkable agreement between our theoretical predictions and the experimental curve. The experimentally determined material parameters used in the present calculation are summarized in Table I. A background contribution, taken to be constant over the frequency range of the d band, was subtracted in Fig. 4. The lack of experimental data on several material constants leaves us with three adjustable parameters: the electron-phonon coupling constant α , the band mass m_b , and the density of charge carriers. These parameters were chosen as follows.

(i) A set of theoretical optical absorption spectra were generated for different values of the band mass and densities (for $m_b = 0.1, 0.2, 0.5, 0.8, 1.0, 2.0$ and $n = \{0.1, 0.2, 0.5, 1.0, 1.2, 1.5, 2.0\} \times 10^{17} \text{ cm}^{-3}$).

(ii) For each of those spectra, the coupling constant α was chosen so as to fit the tail region of the experimental optical absorption spectrum best, using a least-squares fitting procedure (the tail region is relatively insensitive to many-polaron effects).

(iii) The best fitting curve, using again a least-squares evaluation of the goodness of fit, was selected; we found fair agreement with $m_b = 0.5 m_e$ and $n = 1.5 \times 10^{17} \text{ cm}^{-3}$ at $\alpha = 2.1$.

This comparison with experiment could not be performed at higher doping content: the frequency region of the d band usually contains a strong nonuniform contribution of other optical absorption features (such as the onset of the MIR, the tail of the Drude contribution, and the IRAV and phonon modes). To take these other contributions into account, additional adjustable parameters would have to be introduced making a comparison less convincing. Fortunately, experimental results are available in the form of the normalized first frequency moment of the optical absorption spectrum (after subtraction of the MIR and CT bands) $\text{Re}[\sigma_{\text{exp}}(\omega)]$:

$$\langle \omega \rangle = \frac{\int_0^{\omega_{\text{max}}} \omega \text{Re}[\sigma_{\text{expt}}(\omega)] d\omega}{\int_0^{\omega_{\text{max}}} \text{Re}[\sigma_{\text{expt}}(\omega)] d\omega}, \quad (27)$$

where $\omega_{\text{max}} = 10\,000 \text{ cm}^{-1}$.⁵ Lupi *et al.*⁵ determined $\langle \omega \rangle$ for NCCO samples with a varying cerium doping content. Increasing the cerium doping will inject electrons in the copper-oxide planes of the material and increase the 2D charge carrier density in these planes. A comparison of this experimental normalized first frequency moment to the theoretical one presents the advantage that fewer parameters need to be adapted: only the density and the electron band mass have to be taken from experiment or (if experimental values are lacking) fitted.

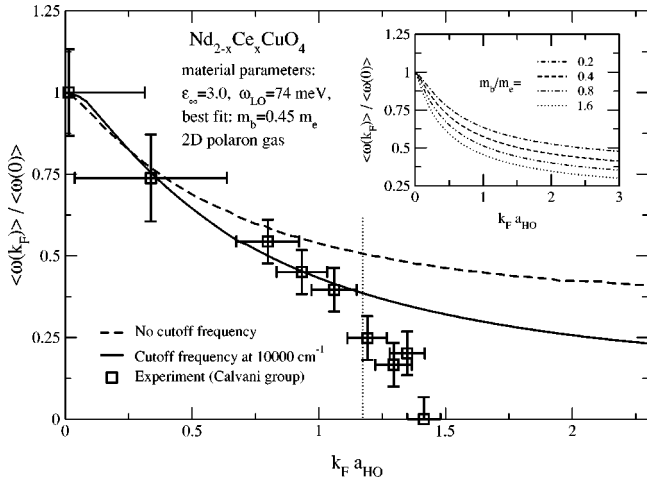


FIG. 5. The normalized first frequency moment of the optical absorption spectra is shown as a function of the density (expressed through the Fermi wave vector). The squares represent the experimental results of Lupi *et al.* (Ref. 5) in a family of $\text{Nd}_{2-x}\text{Ce}_x\text{CuO}_4$ materials. The dashed curve shows the results from the theoretical two-dimensional many-polaron optical absorption, obtained by integrating all frequencies in the calculation of the first frequency moment. The solid curve shows the theoretical results obtained by integrating up to a cutoff frequency, which is chosen at $10\,000\text{ cm}^{-1}$ and which corresponds to the maximum frequency in the experiment (Ref. 5). The material parameters are listed in the figure, and the effect of choosing a different electron band mass is illustrated in the inset. The points with $x < 0.12$, to the left of the vertical dotted line, show agreement with the theoretical result from the many-polaron theoretical optical absorption, but it is clear that the experimental cutoff frequency has to be taken into account. For the samples with $x > 0.12$, a discrepancy between the theoretically predicted first frequency moment and the observed first frequency moment is consistent with a possible insulator-to-metal transition at $x = 0.12$ (Ref. 8).

The carrier density can be estimated numerically from the effective carrier concentrations in the different samples⁵ and from a measurement of the two-dimensional Fermi velocity performed for one of the samples.¹³ As for the other cuprates, the band mass of the electrons in NCCO has not yet been determined experimentally³⁵ and remains as an adjustable parameter.

Figure 5 represents the comparison between the present theory and experiment. The squares with error bars show the experimental results for differently doped samples of NCCO, reported in Ref. 5. The dashed curve shows the normalized first frequency moment of the theoretical optical absorption spectrum, integrated over the entire frequency range ($\omega_{\text{max}} \rightarrow \infty$). The tail region of the many-polaron optical absorption still carries a significant weight, just as it does in the one-polaron optical absorption. It is necessary to include the cutoff frequency. The solid curve represents the theoretical first frequency moment with a cutoff frequency $\omega_{\text{max}} = 10\,000\text{ cm}^{-1}$, which corresponds to the experimental cutoff.⁵

There exists a fair agreement between the theoretical and the experimental values of the normalized first frequency moment for the five samples with lowest density, which have

a cerium doping content of $x < 0.12$. These correspond to the squares to the left of the dotted vertical line in Fig. 5. For the four remaining samples ($x > 0.12$) a discrepancy between the theoretically predicted first frequency moment for unpaired polarons and the observed first frequency moment appears. It has been observed experimentally that the weight of the low-frequency component in these samples (with $x > 0.12$) is significantly larger than the corresponding weight in samples with $x < 0.12$.⁸ This was interpreted in Ref. 8 as a consequence of an *insulator-to-metal* transition taking place around the cerium-doping level of $x = 0.12$. Therefore, it seems reasonable to assume that above this doping level x a change in the nature of the charge carriers takes place. One could hypothesize that, as the formation of bipolarons is stabilized with increasing density of the polaron gas,³⁶ bipolarons start playing a role in the optical absorption spectrum. In a variety of other cuprates and manganates, the presence of bipolarons has also been invoked to interpret a number of response-related properties.³⁷

IV. CONCLUSIONS

Starting from the many-polaron canonical transformations and the variational many-polaron wave function (LDB) introduced in Ref. 2 we have derived a formula for the optical absorption coefficient $\text{Re}[\sigma(\omega)]$ of a many-polaron gas. We find that $\text{Re}[\sigma(\omega)]$ can be expressed in a closed analytical form in terms of the dynamical structure factor $S(q, \omega)$ of the electron (or hole) system, Eq. (24) in 2D and Eq. (23) in 3D. In the present approach, the electron-phonon coupling and the electron-electron many-body effects formally decouple in the expression for $\text{Re}[\sigma(\omega)]$. Therefore, the many-body effects in the electron (hole) system can be taken into account by employing any desired approximation to the dielectric response (Hartree-Fock, RPA, etc.) of this electron (hole) system.

In the present work, the dynamical structure factor $S(q, \omega)$ of the electron (or hole) gas was considered both in the Hartree-Fock and the RPA approximation.

The main effect of the Pauli exclusion principle on the optical absorption of the polaron gas turns out to be a shift of the oscillator strength towards higher frequencies. This effect can be understood in terms of the available initial and final states in the polaron-photon scattering process and naturally invokes the Fermi energy E_F of the electron (hole) gas.

The main effects in the case of the RPA approximation are an overall reduction of the optical absorption at frequencies $\omega > \omega_{LO}$ and the introduction of a novel absorption feature which we identified as a plasmon-phonon peak. This plasmon-phonon peak shifts to higher frequencies with increasing density, such that a double peak structure can appear in the 3D many-polaron optical absorption spectrum, consistent with the observed bimodal polaronic band in cadmium oxide.³⁸

As a first application of the method presented here, we chose to investigate the optical absorption of the interacting polaron gas in the RPA framework. For $\text{Nd}_2\text{CuO}_{4-\delta}$ ($\delta < 0.004$), similarities were observed (see Fig. 4) between the line shape of the experimental d band and the many-polaron

optical absorption as calculated here. To study the density dependence, measurements (performed by Lupi *et al.*⁵ for a family of $\text{Nd}_{2-x}\text{Ce}_x\text{CuO}_4$ materials) of the first frequency moment of the optical absorption were compared to the results of the present theory. We find a fair agreement for the samples with the lowest densities (cerium doping $x < 0.12$). A softening of the first frequency moment of the optical absorption for the samples with higher densities (cerium doping $x > 0.12$) is consistent with a change in the nature of the charge carriers at a doping content $x = 0.12$ inferred in Ref. 8 from infrared absorption experiments.

ACKNOWLEDGMENTS

The authors would like to acknowledge S. N. Klimin and V. M. Fomin for helpful discussions and intensive interactions. We are indebted to P. Calvani for fruitful discussions and for communication of experimental data. We thank F.

Brosens and L. F. Lemmens for discussions. One of us, J.T. (“Postdoctoraal Onderzoeker van het Fonds voor Wetenschappelijk Onderzoek–Vlaanderen”), was supported financially by the Fonds voor Wetenschappelijk Onderzoek–Vlaanderen (Fund for Scientific Research–Flanders). Part of this work was performed in the framework of the “Interuniversity Poles of Attraction Program–Belgian State, Prime Minister’s Office–Federal Office for Scientific, Technical and Cultural Affairs” (“Interuniversitaire Attractiepolen–Belgische Staat, Diensten van de Eerste Minister–Wetenschappelijke, Technische en Culturele Aangelegenheden”), and in the framework of FWO Project Nos. 1.5.545.98, G.0287.95, 9.0193.97, WO.025.99N, and WO.073.94N (Wetenschappelijke Onderzoeksgemeenschap, Scientific Research Community of the FWO on Low Dimensional Systems, “Laagdimensionale systemen”), and in the framework of Project Nos. BOF NOI 1997 and GOA BOF UA 2000 of the Universiteit Antwerpen.

-
- ¹J. T. Devreese, J. De Sitter, and M. Goovaerts, *Phys. Rev. B* **5**, 2367 (1972); see also J. T. Devreese, in *Encyclopedia of Applied Physics*, edited by G. L. Trigg (VCH, New York, 1996), Vol. 14.
- ²L. F. Lemmens, J. T. Devreese, and F. Brosens, *Phys. Status Solidi B* **82**, 439 (1977).
- ³G. Iadonisi, M. L. Chiofalo, V. Cataudella, and D. Ninno, *Phys. Rev. B* **48**, 12 966 (1993); V. Cataudella, G. De Filippis, and G. Iadonisi, *Eur. Phys. J. B* **12**, 17 (1999).
- ⁴J. T. Devreese, S. N. Klimin, V. M. Fomin, and F. Brosens, *Solid State Commun.* **114**, 305 (2000).
- ⁵S. Lupi, P. Maselli, M. Capizzi, P. Calvani, P. Giura, and P. Roy, *Phys. Rev. Lett.* **83**, 4852 (1999).
- ⁶L. Genzel *et al.*, *Phys. Rev. B* **40**, 2170 (1989); B. Bucher *et al. ibid.* **45**, 3026 (1992); P. Calvani *et al.*, *Europhys. Lett.* **31**, 473 (1995).
- ⁷J. P. Falck, A. Levy, M. A. Kastner, and R. J. Birgeneau, *Phys. Rev. B* **48**, 4043 (1993); P. Calvani *et al.*, *Solid State Commun.* **91**, 113 (1994).
- ⁸S. Lupi, P. Calvani, M. Capizzi, P. Maselli, W. Sadowski, and E. Walker, *Phys. Rev. B* **45**, 12 470 (1992).
- ⁹P. Calvani, M. Capizzi, S. Lupi, P. Maselli, A. Paolone, and P. Roy, *Phys. Rev. B* **53**, 2756 (1996); S. Lupi, M. Capizzi, P. Calvani, B. Ruzicka, P. Maselli, P. Dore, and A. Paolone, *ibid.* **57**, 1248 (1998).
- ¹⁰M. K. Crawford, G. Burns, G. V. Chandrasekhar, F. H. Dacol, W. E. Farneth, E. M. McCarron III, and R. J. Smalley, *Phys. Rev. B* **41**, 8933 (1990).
- ¹¹J.-G. Zhang, X.-X. Bi, E. McRae, P. C. Ecklund, B. C. Sales, and M. Mostoller, *Phys. Rev. B* **43**, 5389 (1991).
- ¹²G. A. Thomas, D. H. Rapkine, S.-W. Cheong, and L. F. Schneemeyer, *Phys. Rev. B* **47**, 11 369 (1993).
- ¹³C. C. Homes, B. P. Clayman, J. L. Peng, and R. L. Greene, *Phys. Rev. B* **56**, 5525 (1997).
- ¹⁴J. T. Devreese and J. Tempere, *Solid State Commun.* **106**, 309 (1998).
- ¹⁵D. Emin, *Phys. Rev. B* **48**, 13 691 (1993).
- ¹⁶D. M. Eagles, R. P. S. M. Lobo, and F. Gervais, *Phys. Rev. B* **52**, 6440 (1995).
- ¹⁷S. Tomonaga, *Prog. Theor. Phys.* **2**, 6 (1947); T. D. Lee, F. E. Low, and D. Pines, *Phys. Rev.* **90**, 297 (1953).
- ¹⁸T. D. Lee, L. F. Low, and D. Pines, *Phys. Rev.* **90**, 297 (1953).
- ¹⁹See, e.g., G. D. Mahan, *Many-Particle Physics* (Plenum Press, New York, 1993), p. 210.
- ²⁰J. T. Devreese, in *Polarons in Ionic Crystals and Semiconductors*, edited by J. T. Devreese (North-Holland, New York, 1972).
- ²¹See, e.g., G. D. Mahan, in *Polarons in Ionic Crystals* (Ref. 19, p. 153).
- ²²J. J. Hopfield, *Phys. Rev.* **139**, A419 (1965).
- ²³A. Ron and N. Tzoar, *Phys. Rev.* **131**, 12 (1963).
- ²⁴V. L. Gurevich, I. G. Lang, and Yu. A. Firsov, *Sov. Phys. Solid State* **4**, 918 (1962).
- ²⁵G. D. Mahan, *Phys. Rev.* **145**, 602 (1966).
- ²⁶W. Huybrechts and J. T. Devreese, *Phys. Rev. B* **8**, 5754 (1973).
- ²⁷X. Wu, F. M. Peeters, and J. T. Devreese, *Phys. Rev. B* **31**, 3420 (1985); F. M. Peeters and J. T. Devreese, *ibid.* **36**, 4442 (1987).
- ²⁸X. Wu, F. M. Peeters, and J. T. Devreese, *Phys. Rev. B* **34**, 2621 (1986); *Phys. Status Solidi B* **133**, 229 (1986).
- ²⁹M. Cardona, *J. Phys. Chem. Solids* **24**, 1543 (1963); R. J. Collins and D. A. Kleinman, *ibid.* **11**, 190 (1959); W. Baer, *Phys. Rev.* **154**, 785 (1967); see also E. Kartheuser, in *Polarons in Ionic Crystals and Semiconductors*, edited by J. T. Devreese (North-Holland, New York, 1972).
- ³⁰P. Calvani (private communication); see also Alonso, S. Tortosa, M. Garriga, and S. Piñol, *Phys. Rev. B* **555**, 3216 (1997).
- ³¹For example, A. Isihara, *Electron Liquids* (Springer-Verlag, Berlin, 1993); or G. D. Mahan, *Many-Particle Physics* (Plenum Press, New York, 1993).
- ³²J. T. Devreese, L. F. Lemmens, and J. Van Royen, *Phys. Rev. B* **15**, 1212 (1977).
- ³³S. Fratini and P. Quemerais, *Mod. Phys. Lett. B* **12**, 1003 (1998).
- ³⁴S. Fratini, F. de Pasquale, and S. Ciuchi, *Phys. Rev. B* **63**, 153101 (2001).
- ³⁵J. T. Devreese, in *Models and Phenomenology for Conventional*

- and High-Temperature Superconductivity*, edited by G. Iadonisi, J. R. Schrieffer, and M. L. Chiofalo (IOS Press, Amsterdam, 1999), pp. 287–304.
- ³⁶A. A. Shanenko, M. A. Smondyrev, and J. T. Devreese, *Solid State Commun.* **98**, 1091 (1996).
- ³⁷A. S. Alexandrov, V. V. Kabanov, and N. F. Mott, *Phys. Rev. Lett.* **77**, 4796 (1996); A. S. Alexandrov and A. M. Bratkovsky, *Phys. Rev. B* **60**, 6215 (1999); D. Emin, *ibid.* **45**, 5525 (1992); A. S. Alexandrov and J. Ranninger, *ibid.* **23**, 1796 (1981).
- ³⁸H. Finkenrath, N. Uhle, and W. Waidelich, *Solid State Commun.* **7**, 11 (1969).